

Nano-cluster Controlled Precipitation in Al-Cu and Al-Mg-Si Alloys Containing Microalloying Elements

T. Sato¹, K. Hirose², S. Hirosawa¹

1 Department of Metallurgy and Ceramics Science, Tokyo Institute of Technology, 2-12-1, O-okayama, Meguro-ku, Tokyo 152-8552, Japan

2 Graduate student, Department of Metallurgy and Ceramics Science, Tokyo Institute of Technology, 2-12-1, O-okayama, Meguro-ku, Tokyo 152-8552, Japan

Keywords: Al-Cu alloy, Al-Mg-Si alloy, microalloying, cluster, GP zone, precipitation, AP-FIM,

Abstract

The formation behaviour of nano-clusters in age-hardenable Al-Cu and Al-Mg-Si alloys containing microalloying elements was investigated using TEM and 3D-AP techniques. Hardness and electrical resistivity measurements and a computer simulation method were also performed. In the Al-Cu alloys containing Mg and Ag, Cu/Mg and Cu/Mg/Ag nano-clusters were found to exist by the 3D-AP technique and confirmed to be quite effective to control precipitate microstructures of Al-Cu alloys. A new type GP₁₁₁ zone was formed on the {111} matrix planes by the assistance of nano-clusters. In Al-Mg-Si alloys containing Cu and Ag, the age-hardening behaviour was influenced by the microalloying elements, i.e. the initial stage was suppressed whereas the subsequent stage was accelerated by the microalloying of Cu and Ag. The behaviour was also well understood by taking into account the formation of nano-clusters such as Mg/Ag.

1. Introduction

It has been realized that the nanoscale clusters (*i.e.*, nano-clusters) are generally formed in the initial stage of phase decomposition and are extremely important to control precipitate microstructures of age-hardenable aluminium alloys. Microalloying elements are expected to affect both the formation kinetics and structures of nano-clusters. In our previous papers[1-3], the formation behaviour of nano-clusters was examined using electrical resistivity change, calorimetry, TEM and a computer simulation. In this work we performed the 3D-AP technique together with TEM to detect nano-clusters directly in the typical age-hardenable Al-Cu and Al-Mg-Si alloys containing several microalloying elements such as Mg, Ag, Cu and Zn. Several types of nano-clusters containing solute and microalloying atoms were found. It is also assumed that these nano-clusters strongly interact with quenched-in excess vacancies. The nano-clusters are expected to act as effective heterogeneous nucleation sites for the subsequent precipitates and affect microstructures and resultant alloy properties. In this work the role of microalloying elements on the nano-cluster formation and heterogeneous nucleation behaviour are discussed.

2. Experimental Procedures

Al-3.7%Cu, Al-3.7%Cu-0.29%Mg and Al-4.1%Cu-0.28%Mg-1.03%Ag alloys (in mass%) were prepared for the Al-Cu alloy system. Al-0.83%Mg-0.51%Si, Al-0.83%Mg-0.48%Si-0.27%Cu and Al-0.81%Mg-0.51%Si-0.38%Ag (in mass%) were also prepared for the Al-Mg-Si alloy system. The alloy ingots were homogenized and hot- and cold-rolled to sheets. All the specimens were solution treated and then quenched into iced-water before several aging treatments. TEM observation was performed using a JEM3010 microscope. For 3D-AP observation sharp needle-shaped specimens were carefully prepared and examined using a new 3D-AP machine (Polaron CVT Ltd/Oxford nanoScience Ltd) at 20K. The atom distribution were analysed by the "PoSAP" software.

3. Results and Discussion

3.1 Al-Cu Alloys

3.1.1 Effects of Microalloying Elements

The age-hardening curves for Al-Cu alloys containing microalloying elements of Mg and Ag are shown in Figure 1. The characteristic increase in hardness is found for Al-Cu binary and Mg or (Mg+Ag)-added alloys in Figure 1(a). In the Mg-added alloy the age-hardening is suppressed in the initial stage of aging at RT and then accelerated in the subsequent stage compared with the Al-Cu alloy. At the aging temperature of 373K (Figure 1(b)) the age-hardening of the Mg-added alloy is greatly accelerated from the beginning of aging. On the other hand, the age-hardening of the (Mg+Ag)-added alloy is much suppressed in the initial stage and subsequently greatly accelerated compared with other two alloys. The tendency is more pronounced at 373K. The Ag-added alloy (single addition) exhibited almost similar age-hardening curves to those of the Al-Cu alloy, suggesting that the single addition of Ag causes almost no influence on age-hardening kinetics. TEM micrographs and corresponding diffraction patterns for the Al-Cu and Mg-added alloys aged at RT for 18ks are shown in Figure 2. An imaging plate was used to record the weak intensity of diffraction patterns precisely for both alloys. The

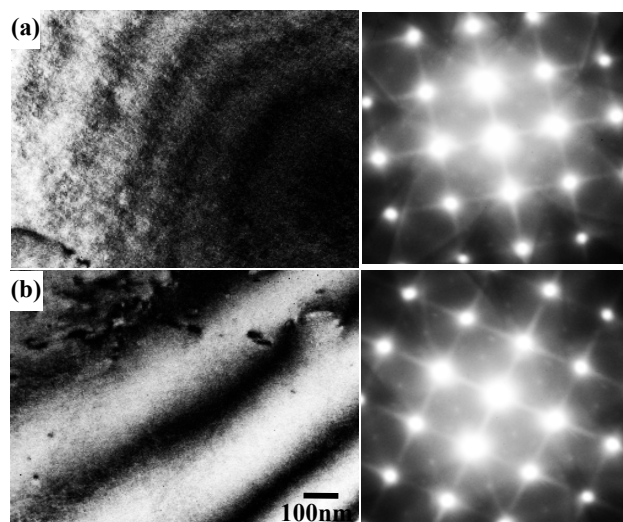
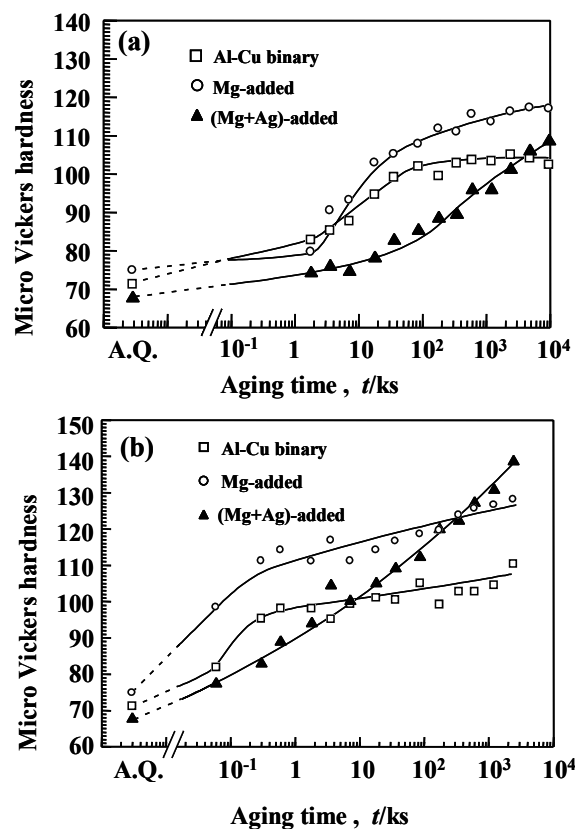


Figure 2: TEM micrographs and corresponding diffraction patterns for (a) Al-Cu and (b) Mg-added alloys aged at RT for 18ks.

Figure 1: Age-hardening curves for Al-Cu binary, Mg-added and (Mg+Ag)-added alloys aged at (a) RT (room temperature) and (b) 373K.

diffraction patterns of both alloys exhibit streaks running towards the $\langle 100 \rangle$ matrix directions, showing that GP zones are formed at this aging stage. The quantitative analysis of the streaks of both alloys revealed that the streaks of the Mg-added alloy was more broad than those of the binary alloy, demonstrating that the GP zones of the Mg-added alloy are much finer than those of the binary alloy. Mg has the effect to produce finer GP zones and possibly to affect nucleation of GP zones.

In order to know the reason for the greatly increased hardness of the (Mg+Ag)-added alloy aged at 373K, TEM observation was performed. The observed microstructure exhibited fine platelets co-existing with the conventional GP(1) zones aligned to the $\langle 100 \rangle$ directions. The fine platelets seem to be aligned on the $\{111\}$ matrix planes. To confirm this point HREM images were taken from the alloy aged at 373K for 604.8ks and an example is shown in Figure 3. Small platelets with the single layer contrast were observed aligned on the $\{111\}$ matrix planes. The precipitates on the $\{111\}$ planes are fully coherent with the matrix and exhibit strain field contrast. These platelets are named as the GP_{111} zones in this work, which are different from the conventional GP(1) zones. From the above observation the highest hardness is attributed to the characteristic microstructures of the GP_{111} zones on the $\{111\}$ matrix planes, the slip planes of the fcc structure. The combined addition of (Mg+Ag) was found to have the effect to produce fine GP_{111} zones. It is also suggested that the combined addition of Mg and Ag affects the nucleation of the fine $\{111\}$ platelets.

3.1.2 Nano-Clusters

As is discussed in our previous papers [1-3] small clusters with the nano-scale size, nano-clusters, are generally formed in the initial stage of phase decomposition of age-hardenable aluminium alloys. The nano-clusters are expected to affect the formation of GP zones and metastable phases. In this work we have applied the 3D-AP (3-dimensional Atom Probe) technique to detect directly nano-clusters formed in the alloys containing microalloying elements. Figure 4 shows 3D atom maps of Al-Cu and Mg-added alloys aged at RT. The crystal orientations are indicated in the figure. To avoid confusion Cu and Mg atom are only displayed in the maps. In the binary alloy Cu atoms aggregate to form small clusters at RT. The statistic analysis of atom positions revealed that the Cu atoms are no longer distributed homogeneously even in the very initial stage of aging. In the Mg-added alloy Cu and Mg atoms aggregate to form small clusters which are closely correlated. Therefore, Cu and Mg atoms are incorporated inside the nano-clusters. It is also reported that quenched-in excess vacancies are incorporated inside nano-clusters. The nano-clusters containing solute atoms (Cu), microalloying atoms (Mg) and vacancies are named as complex clusters. Based on our computer simulation the complex clusters are found to act as effective nucleation sites for GP zones.

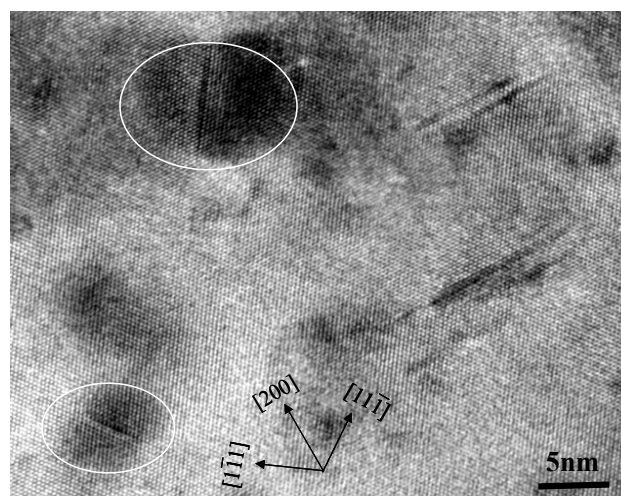


Figure 3: High resolution TEM image showing a new type of GP_{111} zones co-existing with the conventional GP zones in the (Mg+Ag)-added alloy aged at 373K for 604.8ks.

Figure 5 shows 3D atom maps of the binary and (Mg+Ag)-added alloys aged at 373K. In Figure 5(b) some GP zones are observed to be aligned to the $\langle 100 \rangle$ matrix directions. On the contrary, a number of small clusters containing Cu, Mg and Ag atoms are found in Figure (c), (d). In Figure 5(d), some of the clusters are elongated on the $\{111\}$ matrix planes. This indicates that the clusters have the tendency to aggregate on the $\{111\}$ planes and resultantly to accelerate the formation of GP₁₁₁ zones.

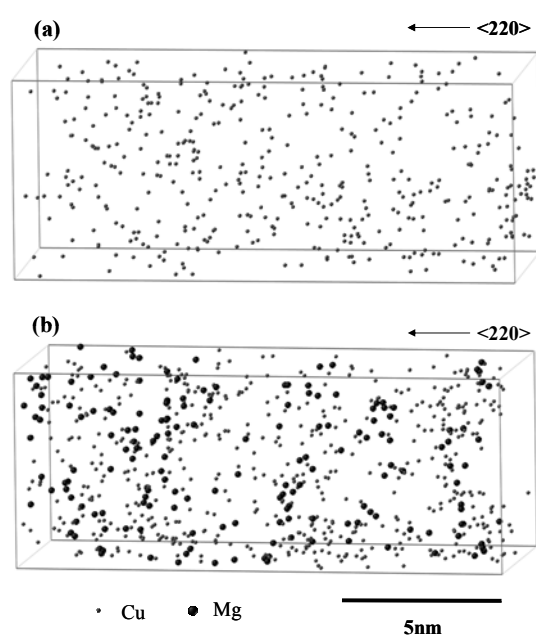


Figure 4: 3D-AP atom maps showing nano-clusters in Al-Cu binary and Mg-added alloys. (a) RT, 21.6 ks, (b) RT, 12.6 ks.

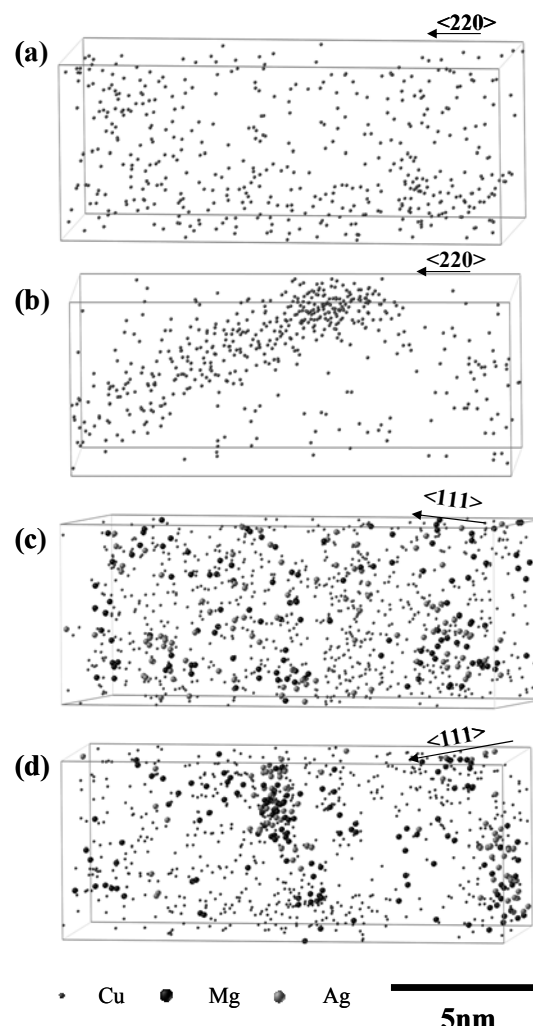


Figure 5: 3D-AP atom maps showing nano-clusters in Al-Cu binary and (Mg+Ag)-added alloys aged at 373K. (a) Al-Cu, 373K for 0.6ks, (b) Al-Cu, 373K for 86.4ks, (c) (Mg+Ag)-added alloy, 373K for 0.6ks, (d) (Mg+Ag)-added alloy, 373K for 86.4ks.

3.1.3 Heterogeneous Nucleation

The nano-clusters containing solute atoms, microalloying atoms and vacancies are expected to act as nucleation sites for the subsequent precipitates. Therefore, to identify the characteristic features of nano-clusters is extremely important. However, to identify nano-clusters experimentally is not easy. Then, we performed a computer simulation to analyse the very early stage of phase decomposition. Figure 6 shows one of the typical examples demonstrating the formation sequence of the complex clusters and nano-clusters. A Mg/vacancy cluster is initially formed (Figure 6(b)), indicating that vacancies are trapped by Mg atoms. In the next step Cu atoms aggregate on the Mg/vacancy cluster

to form a Cu/Mg/vacancy complex cluster (Figure 6(c),(d)). This is an important sequence to represent the heterogeneous nucleation behaviour of GP zones, that is, the nano-cluster assist processing (NCAP) for the GP zone formation. Mg atoms trap vacancies to retard phase decomposition (vacancy trapping) and subsequently aggregate to form Cu/Mg/vacancy complex clusters which accelerate the GP(1) zone formation. Similarly, the (Mg+Ag) combined addition also acts as strong vacancy trap sites in the form of Mg/Ag/vacancy clusters, then contributes to form nano-clusters of Cu/Mg/Ag/vacancy, which effectively act as the nucleation sites for GP₁₁₁ zones formed on the {111} matrix planes (Figure 7). This is again the heterogeneous nucleation of GP zones on nano-clusters.

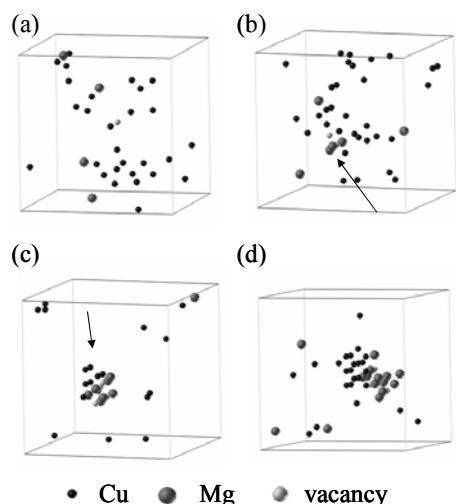


Figure 6: Formation sequence of complex clusters and nano-clusters obtained in the computer simulation for Mg-added alloy. (a) start, (b) 5×10^5 , (c) 5×10^6 and (d) 5×10^8 MCS.

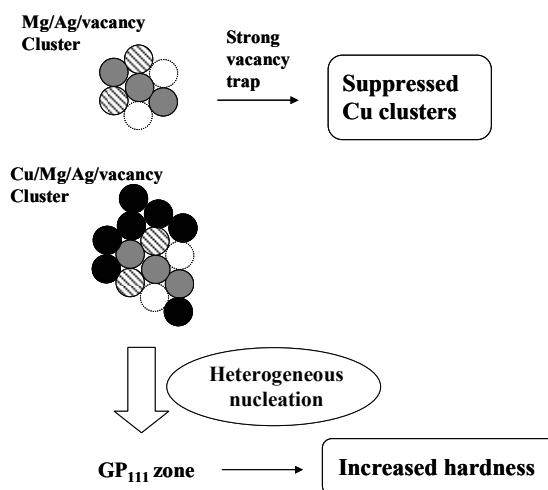


Figure 7: Schematic illustration showing heterogeneous nucleation of GP₁₁₁ zones on nano-clusters.

3.2 Al-Mg-Si Alloys

3.2.1 Effects of Microalloying Elements

Age-hardening curves of Al-Mg-Si alloys containing Cu and Ag at RT are shown in Figure 8. With increasing aging time hardness increases rapidly for Al-Mg-Si, Cu-added and Ag-added alloys. Compared with the Al-Mg-Si alloy, Cu-added and Ag-added alloys show the suppressed age-hardening in the initial stage then accelerated in the subsequent stage. Figure 9 shows age-hardening curves at 453K for single-aged and two-step aged alloys. Two-step aging was performed after pre-aging at RT for 86.4ks. It is clear that Cu and Ag additions enhance the peak hardness in the single aging condition. The TEM micrograph in Figure 10 also demonstrates that the Ag addition produces finer precipitates which are effective to increase hardness.

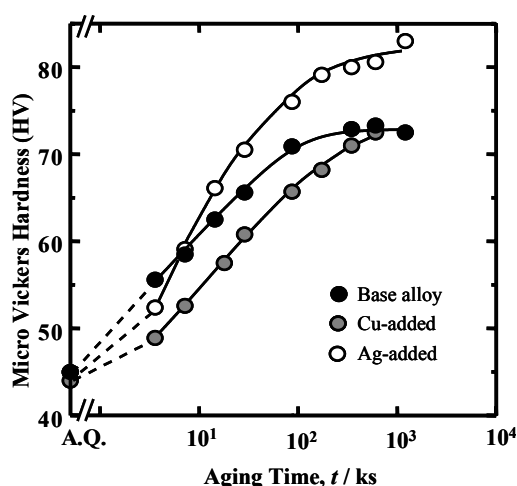


Figure 8: Age-hardening curves for Al-Mg-Si, Cu-added and Ag-added alloys at RT.

The EDX analysis revealed that Ag atoms are much incorporated inside precipitates as shown in Figure 11. It is assumed that Mg/Ag/vacancy clusters are preferentially formed at the beginning of aging as is suggested in Figure 5. The formation of Mg/Ag/vacancy clusters retards the initial age-hardening at RT (Figure 1). In the next stage or at higher aging temperatures, Mg/Ag/vacancy nano-clusters accelerate the formation of GP zones and intermediate phases and increase the peak hardness. In the two-step aging, however, Mg/Ag/vacancy clusters will cause the increased amount of Si-rich clusters at RT and resultantly enhanced negative effect of two-step age-hardening of the alloy (Figure 9).

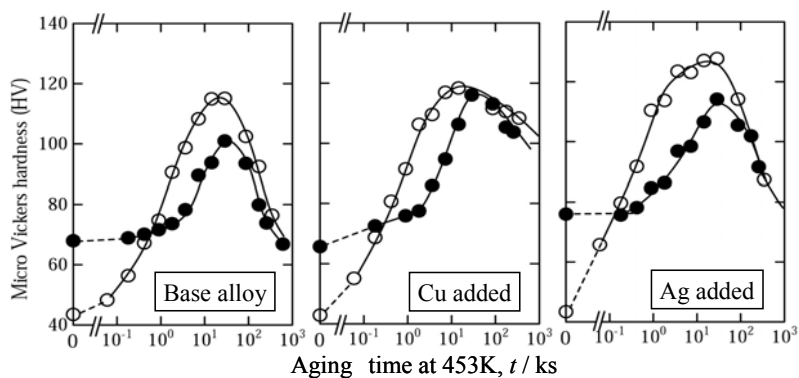


Figure 9: Age-hardening curves for Al-Mg-Si, Cu-added and Ag-added alloys at 453K. Open symbol: single aging at 453K, Solid symbol: two-step aging after pre-aged at RT for 86.4ks.

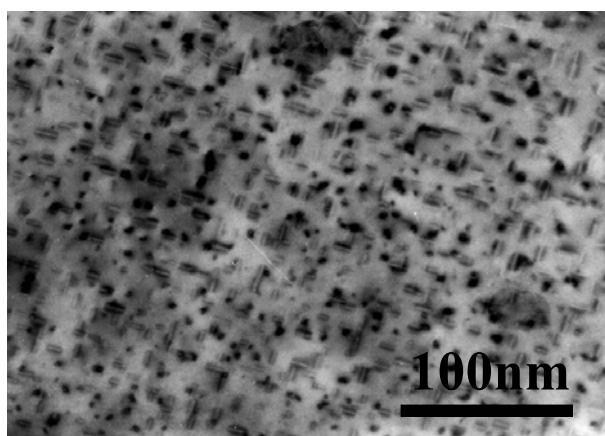


Figure 10: TEM micrograph of Ag-added Al-Mg-Si alloy aged at 453K for 86.4ks.

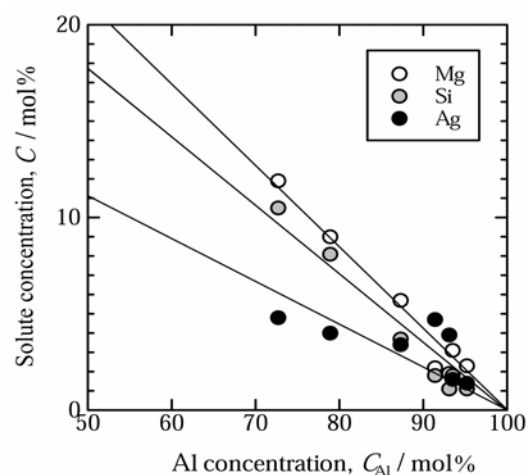


Figure 11: EDX analysis results showing incorporation of Ag atoms inside precipitates shown in Figure 10.

4. Conclusions

- (1) The microalloying elements of Mg and Ag in Al-Cu alloys suppress the initial age-hardening at RT and accelerate the subsequent age-hardening, especially at 373K. The 3D-AP clearly revealed that Cu/Mg and Cu/Mg/Ag nano-clusters are formed. The nano-clusters are effective to accelerate the heterogeneous nucleation of GP zones and a new type of GP₁₁₁ zones.
- (2) The microalloying elements of Cu and Ag in Al-Mg-Si alloys also suppress the initial age-hardening at RT and accelerate the age-hardening at the subsequent stage and at high temperatures. Mg/Ag nano-clusters are assumed to be initially formed and affect the single aging and two-step aging behaviour.

Acknowledgements

The present study was conducted as a part of “Nanotechnology Metal Project” supported by New Energy and Industrial Technology Development Organization (NEDO) and The Japan Research and Development Center for Metals (JRCM).

References

- [1] T. Sato, Materials Science Forum, 331-337, 85-96, 2000.
- [2] K. Hirose, S. Hirosawa and T. Sato, Materials Science Forum, 396-402, 795-800, 2002.
- [3] T. Sato, S. Hirosawa, K. Hirose and T. Maeguchi, Metall. Mater. Trans.,34A, 2745-2755, 2003.